01 Jul 1981

Structural and Magnetic Properties of $Co(urea)_2Cl_2 \cdot 2H_2O$: A Two-dimensional Lsing System with Hidden Canting

Richard Lewis Carlin

Kyong O. Joung

Andries Van Der Bilt

H. den Adel

et. al. For a complete list of authors, see https://scholarsmine.mst.edu/chem_facwork/1729

Recommended Citation

R. L. Carlin et al., "Structural and Magnetic Properties of $Co(urea)_2Cl_2 \cdot 2H_2O$: A Two-dimensional Lsing System with Hidden Canting," *Journal of Chemical Physics*, vol. 75, no. 1, pp. 431-439, American Institute of Physics (AIP), Jul 1981.
The definitive version is available at https://doi.org/10.1063/1.441802

Structural and magnetic properties of $Co(urea)_2Cl_2 \cdot 2H_2O$: A two-dimensional Ising system with hidden canting

Richard L. Carlin, Kyong O. Joung, and A. van der Bilt

Department of Chemistry, University of Illinois at Chicago, Chicago, Illinois 60680

H. den Adel

Kamerlingh Onnes Laboratorium, The University of Leiden, Leiden, The Netherlands

C. J. O'Connor[a] and E. Sinn

Department of Chemistry, University of Virginia, Charlottesville, Virginia 22901
(Received 20 November 1979; accepted 24 June 1980)

The characterization of $Co(urea)_2Cl_2 \cdot 2H_2O$ is reported. The crystal structure at ambient temperatures yields the following information: the chlorine, water, and urea group are coordinated, the urea being bound via the oxygen, to form an octahedral environment about the metal atom. Intermolecular hydrogen bonds between the coordinated chlorine and water ligands produce parallel infinite sheets which provide a two-dimensional exchange pathway. The sheets are separated by the urea ligands and may be considered as magnetically isolated from one another. Crystal data: space group $P2_1/c$, $Z = 2$, $a = 7.397$ (3) Å, $b = 7.795(1)$ Å, $c = 9.764(2)$ Å, $\beta = 116.23(5)$ Å, $V = 505$ Å^3, $\rho_{calc} = 1.87$ g cm^{-3}, $\rho_{obs} = 1.88$ g cm^{-3}, $R = 4.1\%$ for 692 reflections. A λ anomaly in the specific heat was observed at 2.585 ± 0.005 K, and the critical parameters are characteristic of the two-dimensional Ising model. The zero-field susceptibilities have been measured over the temperature interval 1.2–30 K, and are consistent with antiferromagnetic ordering at 2.52 ± 0.05 K. The easy axis lies parallel to the monoclinic a axis, while hidden canting was observed parallel to the b axis. All the data have been analyzed consistently by the two-dimensional Ising model with the parameters $g_a = 7.0 \pm 0.1$, $J/k_B = -2.1 \pm 0.05$ K.

There has been a great deal of interest recently in discovering new examples of the several magnetic model systems.[1,2] There are several aspects to this area of research. First, the spin Hamiltonian generally used to describe magnetic superexchange interactions is written as

$$\mathcal{H} = -2\sum[J_{\parallel} S_{iz} S_{jz} + J_{\perp}(S_{ix} S_{jx} + S_{iy} S_{jy})] , \qquad (1)$$

where the summation over interacting spins on ions i and j is restricted to nearest neighbors. Thus, the concept of lattice dimensionality arises immediately, for one may consider those neighbors which lie either in a linear chain (one-dimensional), plane (two-dimensional), or three dimensional array about the ith reference ion. There is a large number of examples of each of these systems.

Secondly, the spin dimensionality, which is entirely independent of the lattice dimensionality, is defined by the components which enter Eq. (1). When $J_{\parallel}$ and $J_{\perp}$ are equal, the system exhibits isotropic magnetic behavior, and this situation is called the Heisenberg model. When $J_{\parallel}$ and $J_{\perp}$ are found not to be equal, anisotropy occurs and is usually described in terms of two limiting cases. The first, $J_{\parallel} = 0$ but $J_{\perp} \neq 0$, is called the XY model, while the Ising model refers to the case when $J_{\parallel} \neq 0$, $J_{\perp} = 0$. Although many real systems are not expected to exhibit such extreme anisotropy, it is remarkable how many systems can be analyzed in terms of the theory for the limiting behavior. Indeed, one notes for example that in the case of the only three-dimensional XY magnetic system known, $[Co(C_5H_5NO)_6](NO_3)_2$, that the derived exchange constant J/k_B takes the value $-0.228(4)$ K when analyzed in terms of the pure XY model, and changes only to $-0.220(4)$ K when the more realistic ratio $J_{\parallel}/J_{\perp} = 0.31$ is used.[3]

Finally, despite the large numbers of examples of the various magnetic model systems which exist, one continues to search for systems which are better examples: more anisotropic, less anisotropic, better linear chain, etc. An important aspect of this search is to find systems which order at low temperatures, for then such experimental observables as the magnetic specific heat can be determined to higher accuracy; this is due to the smaller phonon heat capacity at lower temperatures. In this regard, we observe that two of the best examples of the two-dimensional Ising model have rather high transition temperatures T_c: K_2CoF_4 orders at 107 K, while Rb_2CoF_4 orders at 101 K.[4]

We report here a characterization of another two-dimensional Ising system, $Co(urea)_2Cl_2 \cdot 2H_2O$, which promises to be of further interest because of its much lower transition temperature of 2.5 K. The crystal structure is reported, along with the measurement and interpretation of the zero-field magnetic susceptibilities and specific heat. As with most cobalt(II) systems at low temperatures,[1-4] the analysis may be carried out in the effective spin $S = 1/2$ formalism. This means that the anisotropic properties arise from the action of the crystalline field rather than from an anisotropy in the exchange interaction.

I. EXPERIMENTAL

The compound $Co(urea)_2Cl_2 \cdot 2H_2O$ has been reported previously.[5] Large single crystals may be obtained by following the published phase diagram.

[a] Current address: Department of Chemistry, University of New Orleans, New Orleans, Louisiana 70122.

 0021-9606/81/130431-09$01.00

TABLE I. Positional and thermal parameters and their estimated standard deviations: $Co(urea)_2(H_2O)_2Cl_2$.[a]

Atom	X	Y	Z	U_{11}, B	U_{22}	U_{33}	U_{12}	U_{13}	U_{23}
Co	0.0000(0)	0.0000(0)	0.0000(0)	0.0150(4)	0.0152(5)	0.0165(4)	−0.0017(4)	0.0090(3)	−0.0015(3)
CL	0.0603(2)	0.0173(2)	0.2706(1)	0.0343(7)	0.0235(6)	0.0197(5)	0.0047(5)	0.0160(4)	0.0020(5)
O(2)	0.3031(5)	0.0602(5)	0.0628(4)	0.022(2)	0.024(2)	0.035(2)	−0.009(2)	0.016(1)	−0.014(2)
O(1)	−0.0956(5)	0.2548(4)	−0.0356(3)	0.018(2)	0.002(2)	0.009(1)	−0.003(2)	0.010(1)	−0.003(1)
N(1)	0.3663(7)	0.2997(7)	0.2086(5)	0.038(2)	0.048(3)	0.054(2)	−0.020(2)	0.029(2)	−0.031(2)
N(2)	0.5736(6)	0.2201(7)	0.0997(5)	0.021(2)	0.047(3)	0.043(2)	−0.017(2)	0.020(2)	−0.014(2)
C	0.4121(8)	0.1889(7)	0.1210(5)	0.022(2)	0.022(3)	0.019(2)	0.002(2)	0.004(2)	−0.002(2)
H(O11)	−0.037(10)	0.308(9)	−0.070(7)	2.(2)					
H(O12)	−0.073(9)	0.307(8)	0.024(7)	2.(1)					
H(N11)	0.436(10)	0.385(9)	0.246(7)	3.(2)					
H(N12)	0.248(12)	0.309(10)	0.209(8)	4.(2)					

[a]The form of the anisotropic thermal parameter is

$$\exp[-2\pi^2 (U_{11}h^2a^{*2} + U_{11}k^2b^{*2} + U_{33}l^2c^{*2} + 2U_{12}hka^*b^* + 2U_{13}hla^*c^* + 2U_{23}klb^*c^*)].$$

Single crystals were oriented for the magnetic measurements by x-ray precession camera techniques. Zero-field susceptibilities were obtained by procedures described earlier.[6,7] Specific heat techniques using the conventional heat pulse method are as previously reported.[8] The carbon thermometer was calibrated below 1.3 K against the vapor pressure of ^3He. The cryostat could be moved into an iron core magnet capable of providing a field of 0.73 T.

Crystal data for $Co(urea)_2(H_2O)_2Cl_2$, $CoCl_2O_4N_4C_2H_{12}$. Molwt 284, space group $P2_1/c$, $Z=2$, $a=7.397(3)$ Å, $b=7.795(1)$ Å, $c=9.764(2)$ Å, $\beta=116.23(5)°$, $V=505$ Å^3, $\rho_{calc}=1.87$ g cm^{-3}, $\rho_{obs}=1.88$ g cm^{-3}, $\mu(MoK\alpha)=22.8$ cm^{-1}.

Refined cell dimensions and their estimated standard deviations were obtained from least squares refinement of 28 accurately centered reflections. The mosaicity of the crystal was examined by the ω-scan technique and judged to be satisfactory.

A. Collection and reduction of the data

Diffraction data were collected as previously described[9] at 297 K on a computer-controlled Enraf–Nonius four-circle CAD-4 diffractometer, using monochromated $MoK\alpha$ radiation. The $\theta-2\theta$ scan technique was used to record the intensities for all nonequivalent reflections for which $1° < 2\theta < 48°$. Scan widths (SW) were calculated from the formula $SW = A + B\tan\theta$, where $A = 0.60°$ and $B = 0.35°$. The raw intensity data were corrected for Lorentz-polarization effects (including the polarization effect of the crystal monochromator) and then for absorption. Of the 760 independent intensities, 692 had $F_0^2 > 3\sigma(F_0^2)$, where $\sigma(F_0^2)$ was estimated from counting statistics.[10] These data were used in the final refinement of the structural parameters.

B. Determination and refinement of the structure

The volume of the unit cell, and the known molecular weight of the complex, require that the metal atom be located on a special position at the origin. The three-dimensional Patterson function calculated from all intensity data confirmed this postulate. The positions of the metal atom and of the three independent ligand donor atoms derived from the Patterson function phased the intensity data sufficiently well to permit location of the other nonhydrogen atoms from a three-dimensional Fourier synthesis. Further Fourier syntheses permitted the location of the hydrogen atoms involved in hydrogen-bonding networks.

Full-matrix least-squares refinement was based on F, as previously described.[11] The atomic scattering factors were taken from the literature.[12] The effects of anomalous dispersion[13] for all nonhydrogen atoms were included in F_c. The principal programs used have been described.[14]

Anisotropic temperature factors were introduced for all nonhydrogen atoms. The hydrogen atom parameters were included for three cycles of least-squares refinement and thereafter held fixed. The model converged with $R = 4.1\%$ and $R_w = 5.9\%$, where the symbols have their usual meanings.[14] A structure factor calculation with all observed and unobserved reflections included gave $R = 4.3\%$; on this basis it was decided that careful measurement of reflections rejected automatically during data collection would not be warranted. A final Fourier difference map was featureless. A table of the observed and calculated structure factors is available.[15]

II. RESULTS AND ANALYSIS

A. Crystal structure

Final positional and thermal parameters for the complex are given in Table I. Tables II and III contain the bond lengths and angles. The digits in parentheses in the tables are the estimated standard deviations in the least significant figures quoted and were derived from the inverse matrix in the course of least-squares refinement calculations. Figure 1 shows the octahedral metal environment in $[Co(urea)_2(H_2O)_2Cl_2]$. The coordinated chlorine atoms are hydrogen bonded to the coordinated water ligands to form two-dimensional sheets which provide a two-dimensional exchange pathway. Part of this hydrogen-bonded $[CoCl_2(H_2O)_2]_\infty$ network is shown as a stereoview of the bc plane in Fig. 2. There are two types of intermolecular $Cl\cdots H_2O$ bond at 3.162(2) Å and 3.217(2) Å, respectively. The difference between them is emphasized in Fig. 2, which shows the 3.217 Å bonds in

TABLE II. Bond distances (Å).

Co	Cl	2.481(1)
Co	O(1)	2.086(1)
Co	O(2)	2.099(1)
C	O(2)	1.255(2)
C	N(1)	1.360(3)
C	N(2)	1.322(3)
O(1)	H(O11)	0.78(3)
O(1)	H(O12)	0.67(3)
N(1)	H(N11)	0.82(4)
N(1)	H(N12)	0.88(4)
Cl	O(1)	3.162(2)[a]
Cl	O(1)	3.217(2)[a]
O(2)	N(1)	3.066(2)[a]
Cl	H(O11)	2.40(3)[a]
Cl	H(O12)	2.56(3)[a]

[a]H-bonding distances.

TABLE III. Bond angles (deg).

O(1)	Co	O(2)	94.3(1)
Cl	Co	O(1)	90.8(1)
Cl	Co	O(2)	90.6(1)
Co	O(2)	C	134.5(1)
O(2)	C	N(1)	120.3(2)
O(2)	C	N(2)	121.4(2)
N(1)	C	N(2)	118.4(2)
Co	Cl	O(1′)	136.6(1)[a]
Co	Cl	O(1)	137.3(1)[a]
Co	O(2)	N(1)	116.7(1)[a]
Cl	H(O11)	O(1)	166(1)[a]
Cl	H(O12)	O(1)	169(1)[a]
O(2)	H(N11)	N(1)	158(1)[a]

[a]Hydrogen-bonding angles.

the plane of the page, while the 3.162 Å bonds are shown running slightly into the page and are foreshortened. However, the difference between these hydrogen bond distances is quite small in terms of exchange pathways. The two-dimensional sheets are further linked by hydrogen bonding between the urea ligands [involving O(2) and N(1)] above and below the sheets. The urea ligands serve to separate adjacent $[CoCl_2(H_2O)_2]_\infty$ sheets and to isolate them magnetically, as is illustrated in Fig. 3.

B. Specific heat

A collection of several crystals which had grown clustered to each other was powdered in order to measure the specific heat between 1 and 90 K. The time which the sample needed to reach thermal equilibrium after a heat pulse was only 30 s at low temperatures and increased to 3 min at 90 K. We observed that when the specific heat increased, the time to reach equilibrium also increased. We estimate that in the helium temperature region the thermal relaxation time between the sample holder and the thermometer is of the order of 0.01 s; so the internal heat distribution in the powdered sample must cause the longer relaxation time. Therefore we believe that the temperature in our sample is determined within 5 mK in the helium temperature region.

The results of the specific heat measurements up to 20 K are displayed in Fig. 4; a sharp lambdalike peak at 2.585 ± 0.005 K is apparent. There is another peak

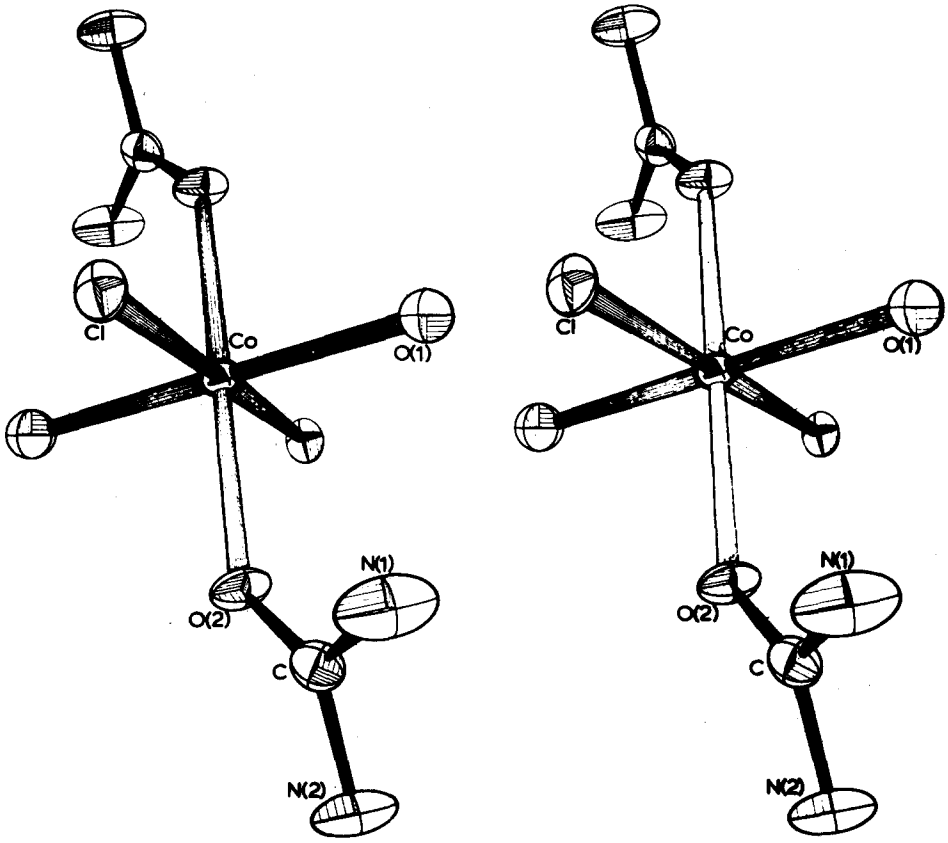

FIG. 1. Stereoscopic pair view of Co $(urea)_2Cl_2(H_2O)_2$ molecule.

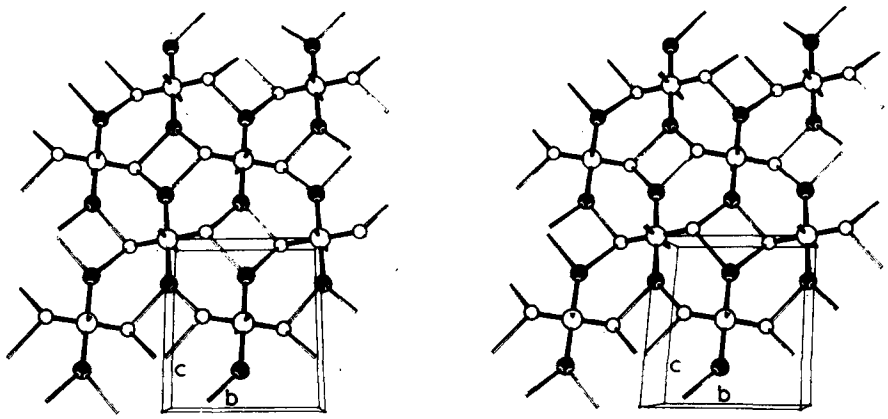

FIG. 2. Stereo view of $[CoCl_2(H_2O)_2]_\infty$ network in *bc* plane. The urea ligands are omitted for clarity. The filled circles are the chlorine atoms.

at 5.95 ± 0.02 K, also of magnetic origin, because it disappears when a relatively low magnetic field of 0.73 *T* is applied to the powdered sample. It is assigned to an unknown impurity. The shape of the main peak changes in the applied field; the peak becomes lower (but also shifts slightly to higher *T*). In order to obtain the same amount of entropy as without any field, the high temperature tail must be larger. This explains why the specific heat in magnetic field at 6 K is slightly larger than without the external field.

Aside from the small impurity contribution, which was subtracted before data analysis, the specific heat consists of two contributions, which we assume to be additive: the lattice and magnetic terms. From the data above 15 K we made an estimation for the lattice contribution. It is decomposed into a sum of Debye and Einstein functions. This is done by a trial and error method, which will be described elsewhere.[16] A nonmagnetic isostructural compound is not yet available. As a simplification we assume a model in which there are two centers for the collective modes of vibration: the urea ligands and the $[CoCl_2(H_2O)_2]$ complex. The one and only noncollective (Einstein) mode is difficult to explain, but has also been found in several other compounds.[16] Our best fit for the lattice was with ${}^{24}\theta_D = 600$ K, ${}^{15}\theta_D = 212$ K, and ${}^{1}\theta_E = 62.5$ K. The lattice contribution below 15 K is extrapolated by calculating the contribution according to the given temperatures.

From the raw data the lattice contribution and the 5.95 K impurity contribution are subtracted. The critical data were obtained by numerical integration of the discrete experimental data, which were corrected for obvious erroneous data. The values of the critical data are given in Table IV, along with a comparison of theoretical results.[17] The lattice entropy below T_c amounts to only 0.2% of S_c/R, while the lattice entropy at 10 K is 8% of S_{10}/R. The lattice contributes to E_c and E_{10}, respectively, 0.2% and 20%. These values are a rough indication for the accuracy of the critical data, although the lattice has been subtracted. The total entropy to $T = \infty$ gained in the transition is within 0.5% of the expected value for a magnetic ion with effective spin $S = 1/2$.

Below 1.7 K, *C* was found to be proportional to T^5. This enabled us to make an easier estimation for the entropy below 1 K; it is less than 1% of S_c/R.

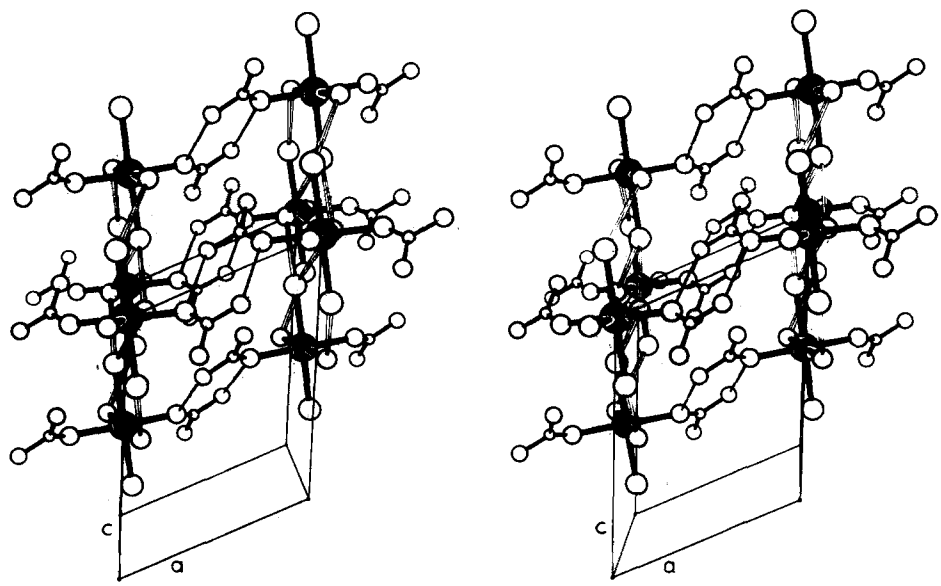

FIG. 3. Stereoscopic side view of the two-dimensional $[CoCl_2(H_2O)_2]_\infty$ sheets (in the *bc* plane), showing the hydrogen bonding between the sheets via the urea ligands in the *a* direction.

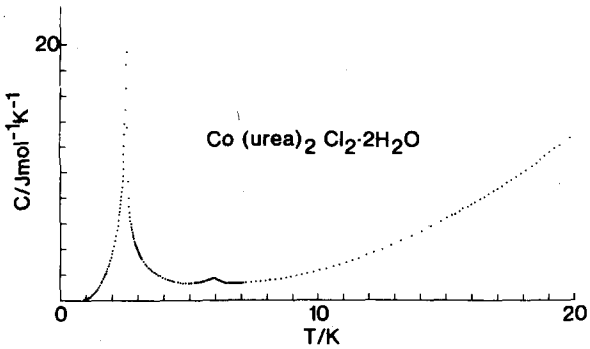

FIG. 4. Specific heat (0–20 K).

TABLE IV. Critical data values.

	$Co(urea)_2Cl_2 \cdot 2H_2O$	2*D* Ising triangular lattice	2*D* Ising square lattice
$\frac{S_c}{R}$	0.337	0.330	0.306
$\frac{S_\infty - S_c}{R}$	0.353	0.363	0.387
$\frac{E_0 - E_c}{RT_c}$	0.282	0.275	0.258
$\frac{-E_c}{RT_c}$	0.69(2)	0.549	0.623

C. Zero-field susceptibilities

The susceptibilities were measured in zero applied field between 1.2 and 30 K in four orientations: parallel to the *a* and *b* axes of the monoclinic crystal, as well as two other directions in the *ac* plane. One orientation, c^*, was chosen perpendicular to the *a* and *b* axes, while the other, the *a'* axis, was chosen at 10° away from *a*, towards c^*. The data are illustrated in Fig. 5.

The *b* axis is a principal axis of the susceptibility tensor for a monoclinic system. The two further principal axes must lie in the *ac* plane, and correspond to directions of maximum and minimum susceptibility. The data below 3 K indicate that the *a* axis is in fact the antiferromagnetic axis of preferred alignment, for the susceptibility exhibits a broad maximum and then drops toward zero value at low temperatures. The critical temperature $T_c(0)$ at which $\partial\chi_a/\partial T$ has a maximum value was found to be 2.52 ± 0.05 K. If the *a* and c^* axes are the two remaining principal axes of the susceptibility tensor, then one should be able to calculate the *a'*-axis data from the values of χ_a, χ_{c^*}, and the geometry of the system. This was indeed found to be so: $\chi_{a'} = \chi_a \cos^2 10 + \chi_{c^*} \sin^2 10$. The data also show that the c^* axis is the hard or perpendicular axis of an ordered antiferromagnet. The impurity which yielded the specific heat peak at 5.95 K is at too low a concentration to affect noticeably the susceptibilities at that temperature.

The data observed parallel to the *b* axis exhibit a very sharp peak at about 2.57 ± 0.02 K, and then drop to a nonzero value at low temperatures. This is behavior typical of a weak ferromagnet: the magnitude of χ_b is observed to be too large for that of a simple antiferromagnet, and too small to suggest ferromagnetism. No absorption (χ'') was noted in χ_b over the whole measured

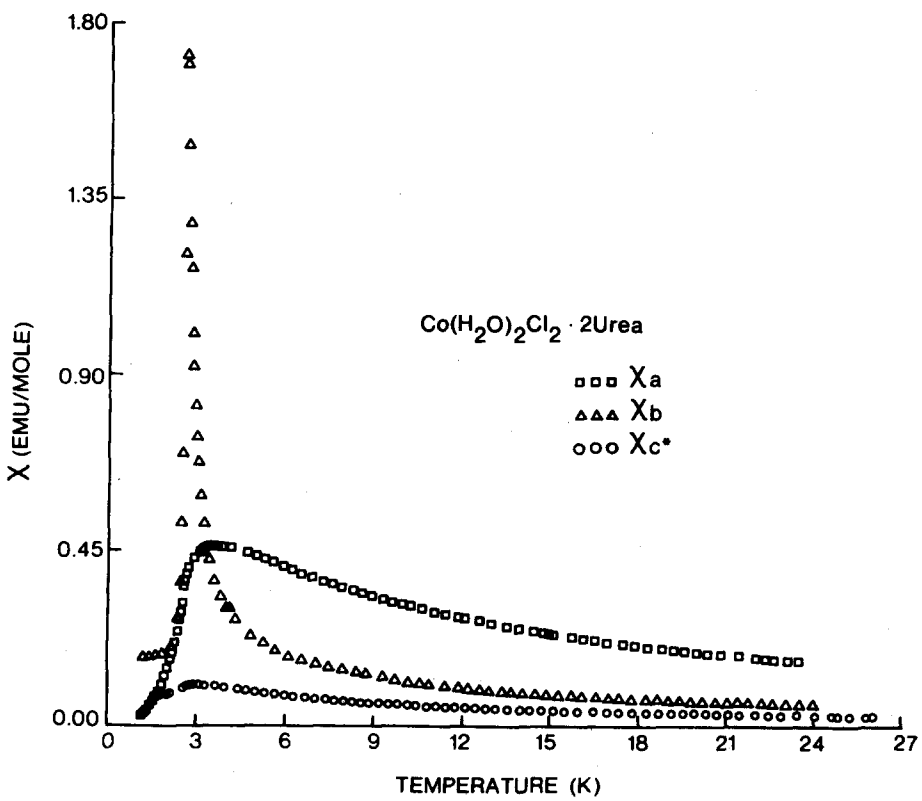

FIG. 5. The susceptibilities measured along the *a*, *b*, and c^* axes as a function of temperature.

TABLE V. Curie–Weiss fits at high temperatures for $Co(urea)_2Cl_2 \cdot 2H_2O$.

	g	θ(K)
χ_a	7.3±0.1	−6.0±0.05
χ_b	4.0±0.05	−3.6±0.05
χ_c*	2.9±0.1	−5.2±0.1

temperature interval. Although the susceptibility is large, it is still much less than the reciprocal of the demagnetizing factor for the particular sample. The result is similar to that recently reported[18] for χ_a of Co(1, 2,4-triazole)$_2$(NCS)$_2$, where it was shown that such behavior is characteristic of a system with hidden canting.

These data have been fit in two fashions, depending on the temperature interval. All of the data above 10 K, where magnetic exchange effects are not predominant, may be fit excellently by the Curie–Weiss law ($S=1/2$) with the parameters listed in Table V. The Weiss constants are all antiferromagnetic in sign, and the g values sum to 14.2, which is a bit higher than the theoretical expectation that their sum be about 13. A better result would be obtained if data were available to higher temperatures.

Nevertheless, the result accords nicely with what one anticipates in those examples in which cobalt acts as an Ising ion: one g value, g_a in this case, is much larger than the other two, and corresponds to the parallel orientation of the measuring field to the easy axis, the a axis in this case. This fact, together with the nearly perfect quadratic character of the bc plane of the crystal lattice, led us to the second fitting procedure, an attempt to fit χ_a to the theoretical calculations[19–21] for the planar Ising lattice.

The χ_a data were simultaneously fit to three different theoretical results, each derived for a different temperature region of the $2D$ Ising system. The equations used are too lenghthy to reproduce here, but the following procedure was used: The data above 4 K were fitted to Eq. (3.1) of Ref. 21, which is a high-temperature expansion for the plane square lattice. The data over the temperature interval 2.52–4 K (recall that T_c is 2.52 K) were fitted by Eq. (5.18) of Ref. 19, which is an expansion applicable near the critical point. The data below 2.52 K were fitted by Eq. (6.7) of Ref. 19, which is a low temperature series extrapolation to the critical point for the plane square Ising lattice. As is illustrated in Fig. 6, an excellent fit over the entire measured temperature region was obtained with one set of parameters, $g_a = 7.0 \pm 0.1$ and $J/k_B = -2.1 \pm 0.05$ K. The agreement of the value of g_a obtained from the Curie-Weiss fit is adequate, although the value 7.0 is probably more reasonable.

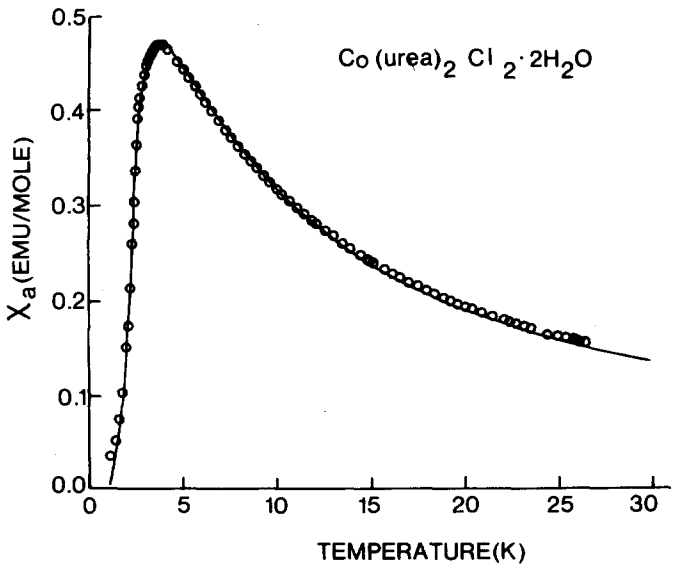

FIG. 6. The susceptibility measured along the a or preferred axis. The points are experimental, the curve is the fit described in the text.

One of the characteristic features of the plane square Ising model[1,19] is that the parallel susceptibility goes through a rather broad maximum above T_c. Fisher[20] calculates that $T_{max}/T_c = 1.5371$, and our experimental result for this ratio in χ_a of $Co(urea)_2Cl_2 \cdot 2H_2O$ is 1.5 ± 0.07. The agreement is excellent. Furthermore, there are several other quantities characteristic of the quadratic Ising lattice which Fisher has derived, and they are compared with our experimental results in Table VI. The agreement again is gratifying. The data along the c^* or perpendicular axis, however, are the smallest measured here, and their temperature variation is quite small. Small misorientation errors and crystal imperfection tend to cause errors in the ratio $\chi_\parallel(\max)/\chi_\parallel(T_c)$ and $\chi_\perp(T_c)/\chi_\perp(0)$, and so we believe that, on the whole, the susceptibility data are well characterized by the plane square Ising model.

III. DISCUSSION

It is clear from the above that $Co(urea)_2Cl_2 \cdot 2H_2O$ is a good example of the planar Ising model of an antiferromagnet. The parameters arising from the specific heat analysis are in reasonable agreement with those anticipated for the quadratic Ising lattice. The analysis of the χ_a data is also consistent with this. What is quite certain is that, irrespective of the particular structure of the lattice, this material is not ordering in the usual three-dimensional fashion. Thus, the smallest S_c calculated[17] for any $3D$ lattice (diamond, $z=4$) is 74% of $R\ln 2$, a value far higher than the 49% observed here. Further-

TABLE VI. Comparison of theoretical results for the quadratic Ising model with experimental values for $Co(urea)_2Cl_2 \cdot 2H_2O$.

	Fisher[a]	Experiment[b]
$\chi_\parallel(\max)/\chi_\parallel(T_c)$	1.552	1.35±0.10
$T_{max}(\parallel)/T_c(\parallel)$	1.5371	1.5±0.07
$\chi_\perp(\max)/\chi_\perp(T_c)$	1.0406	1.08±0.05
$\chi_\perp(T_c)/\chi_\perp(0)$	1.13695	>1.3
$T_{max}(\perp)/T_c(\perp)$	1.08872	1.12±0.05

[a]From Ref. 19. [b]This work.

more, the broad maximum and smooth shape of the χ_a data have already been noted.

Several other points concerning the magnetic structure come to mind. The crystal structure shows that the four nearest cobalt neighbors in the *bc* plane form a rectangle rather than a square; the neighbors are separated by 9.76 Å in the *b* direction and 7.795 Å in the *c* direction. Nevertheless, the nearest neighbor superexchange paths are all equivalent and the fit to a quadratic lattice ($J = J'$) is a reasonable one.

In the low temperature tail C is proportional to T^5, which is as expected if the large anisotropy has introduced a gap in the spin-wave spectrum. Predominantly the system seems to be of Ising lattice dimensionality two; the good resemblance of the critical data to those of a triangular two-dimensional system is a case of coincidence, because the structure requires a magnetic coordination of four, so that the square, kagome, or diamond 2*D* Ising lattices remain. The square 2*D* Ising lattice is in favor because deviations from the theoretical and experimental critical data are the smallest of the three possibilities mentioned.

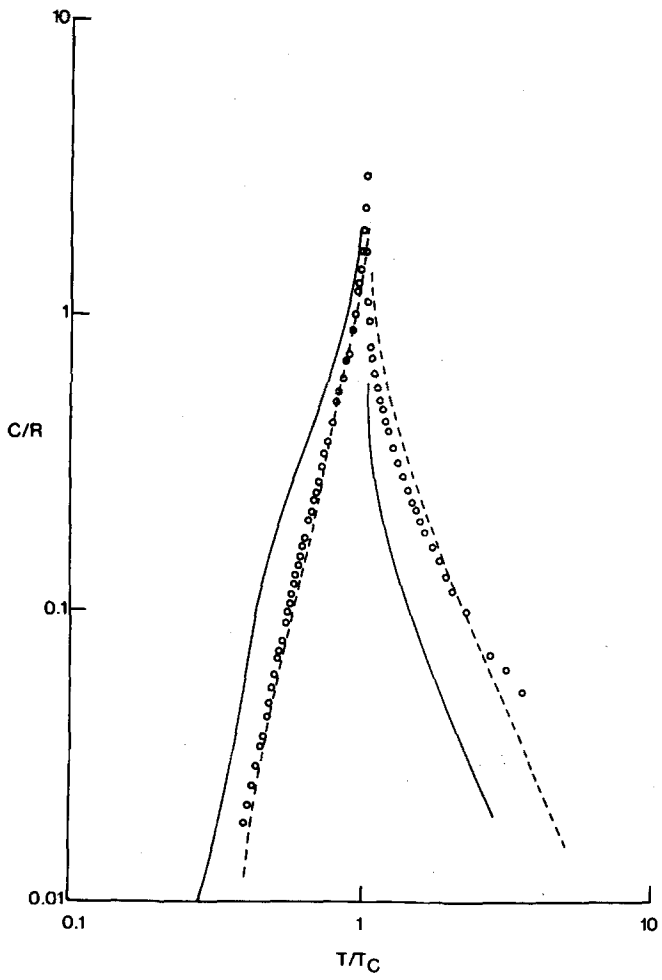

FIG. 7. A plot of C/R versus T/T_c. The points are experimental, the solid curves correspond to the simple cubic 3*D* Ising model, while the dashed curve corresponds to the square 2*D* Ising model.

TABLE VII. Comparison of theoretical results[a] for critical parameters.

	Experimental[b]	Diamond, $z=4$	Simple cubic, $z=6$
A_+	0.238	0.21	0.221
A_-	0.608	0.59	0.51
A_+/A_-	2.55	2.8	2.3
S_c/R	0.337	0.511	0.56
$\frac{E_c - E_0}{RT_c}$	0.282	0.418	0.447

[a]Reference 23. [b]This work.

We neglected the influence of the neighboring layer, separated by the ligands, in the above discussion. This is reasonable, because the distances between the cobalt ions in the layer are much smaller than between the layers. The exchange constant coupled with the interactions between the layers must be quite small. Navarro[22] has calculated the effects when a linear chain crosses over to a 2*D* or 3*D* Ising system. Unfortunately, no such results for crossover from a 2*D* system into a 3*D* one as the temperature decreases are yet available, while we assume that this is the case in this compound. If we compare the experimental specific heat with 2*D* and 3*D* Ising models (Fig. 7), all scaled to T/T_c, we see that below T_c our data are fitted well by the 2*D* Ising calculation; above T_c our data are between 2*D* and 3*D*. (Extra care should be taken for $T/T_c \geq 2$: there will be still some influence of the second peak and secondly the influence of a small error in the estimation of the lattice contribution will be easily seen as a fitting error.)

Another criterion by which to judge this compound is the critical behavior close to T_c. Fisher[23] characterizes the specific heat in the peak region by

$$\frac{C(T)}{R} = A\,|\ln|1 - T/T_c|\,| - A_1 + O\left[(T - T_c)\ln|T - T_c|\right]. \tag{2}$$

If we neglect the last contribution, we get a straight line in a plot of C versus $\ln|1 - T/T_c|$ or two straight lines in the case that one A value (A_+) is found when $T > T_c$, which differs from that when $T < T_c$(A_-). The square 2*D* Ising solution predicts $A_+ = A_- = 0.495$, which is a symmetrical peak. The experimental data display deviations near T_c; the peak is flattened. This could be caused by the method of measuring specific heat by means of finite nonzero temperature changes. This will average the specific heat. We eliminated this effect by changing the heat pulses. Size effects in our powdered and highly compressed sample are unlikely to be dominant.

If we plot C versus $\ln|1 - T/T_c|$ (using $T_c = 2.587K$) the asymmetrical behavior of the experimental data is most striking. For the sake of clarity the line in between the data (Fig. 8) is the 2*D* Ising solution. The values obtained are given in Table VII. This result is unusual: the critical behavior (the A's) suggest that the

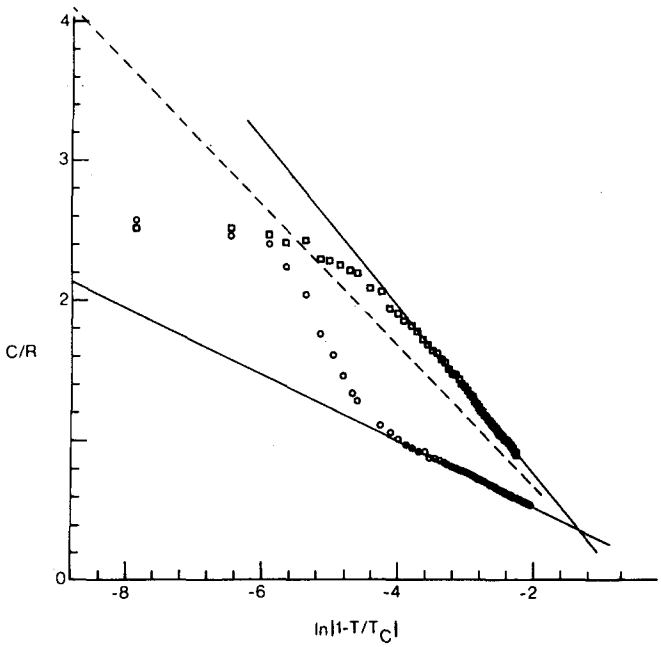

FIG. 8. A plot of C/R versus $\ln|1 - T/T_c|$. The boxes correspond to $T < T_c$ and the circles to $T > T_c$. The dashed line corresponds to the 2*D* Ising solution.

lattice is something between diamond or simple cubic, while the critical data (S_c, E_c) are in contradiction with these models.

If we restrict ourselves to a 2*D* Ising model, but if we introduce anisotropy in the interaction in the layer, the critical behavior changes. The peak becomes asymmetrical. Nevertheless, it is a change in the wrong direction, because for $T > T_c$, C becomes larger than in the isotropic case. In the same way, C below T_c is smaller than in the 2*D* square solution. S_c/R will also be smaller. So introducing anisotropy in the layer is not the right solution.

The lattice dimensionality crossover effects are not expected to be observable in the susceptibility of an antiferromagnet.

Another interesting feature is the observed weak ferromagnetism, which frequently occurs with cobalt systems.[18,24–29] The magnetic moments are primarily antiferromagnetically aligned parallel with the a axis but cant slightly towards the b axis in order to give the observed behavior of χ_b above the transition temperature. When ordering occurs at T_c, the moments in successive bc planes cancel each other's contribution, and hidden canting results. One of the requirements for this phenomenon to occur is that there not be a center of symmetry between neighboring ions. The crystal structure of $Co(urea)_2Cl_2 \cdot 2H_2O$ with two molecules in the monoclinic unit cell guarantees this situation. An examination of the packing diagram in Fig. 2 shows in fact that the urea–Co–urea axis of the metal atom at the origin is cocked with respect to that of its symmetry-related partner. A similar situation was encountered with $Co(CH_3COO)_2 \cdot 4H_2O$,[29] which is also monoclinic ($P2_1/c$) with two inequivalent molecules per unit cell. g-Value anisotropy is required for the antisymmetric exchange of the Dzyaloshinsky–Moriya[24] form $\mathbf{D} \cdot \mathbf{S}_i \times \mathbf{S}_j$ to occur in a cobalt(II) system. That condition is also easily met by this system, for we note that g_a is about 7.0 and $D \propto \Delta g/g$, where $\Delta g = g - 2$.

Nevertheless, another, more likely mechanism exists which can also provide canting. This is the case of large g-value anisotropy combined with a lack of parallalism of the principal axes of the g tensors at neighboring inequivalent sites.[25] Although we have no EPR data on the orientation of the g axes of $Co(urea)_2Cl \cdot 2H_2O$, it is likely that this compound exhibits these properties. Indeed, it has been suggested[30] that cobalt is too anisotropic to follow the Dzyaloshinsky–Moriya behavior, and that the tilting of the g-tensor axes is instead the characteristic mechanism for the canting. One way to distinguish the two possible mechanisms is by measuring the canting angle (by magnetization measurements, NMR, or neutron diffraction) and comparing the result with that calculated from the two models. Unfortunately, we have no such data at this time. We note in several cases[26,29] that the susceptibility remained constant below T_c in the direction of the ferromagnetic moment. The value achieved is the reciprocal of the demagnetizing factor. That a sharp peak is observed here, with the susceptibility dropping precipitously below T_c, suggests that no moment persists below the transition temperature. This is consistent with the fact that no absorption (χ'') was observed, which means that no ferromagnetic domains develop.

One anticipates from earlier studies on other canted systems[18,31] that $Co(urea)_2Cl_2 \cdot 2H_2O$ will behave as a metamagnet in applied magnetic fields. Preliminary results to be reported elsewhere suggest that this is the case.

ACKNOWLEDGMENTS

This research was supported by NSF Grants DMR 76-18963, DMR 7906119, and CHE 77-01372. P. van Liempt assisted with the specific heat measurements. We thank Professor S. A. Friedberg for providing us with a preprint of Ref. 29 and D. W. Engelfriet for a preprint of Ref. 18. We also thank Dr. L. J. de Jongh, Dr. H. A. Groenendijk, and Dr. A. J. van Duyneveldt for their comments. Dr. J. N. McElearney furnished the samples. We also appreciate the perceptive comments of the referee.

[1] L. J. de Jongh and A. R. Miedema, Adv. Phys. 23, 1 (1974).
[2] R. L. Carlin and A. J. van Duyneveldt, *Magnetic Properties of Transition Metal Compounds* (Springer, New York, 1977).
[3] J. Bartolome, H. A. Algra, L. J. de Jongh, and R. L. Carlin, Physica (Utrecht) B 94, 60 (1978).
[4] D. J. Breed, K. Gilijamse, and A. R. Miedema, Physica (Utrecht) 45, 205 (1969).
[5] A. I. Pavlenko, K. S. Sulaimankulov, and V. G. Shevchuk, Russ. J. Inorg. Chem. 15, 1309 (1970).
[6] S. N. Bhatia, R. L. Carlin, and A. Paduan Filho, Physica (Utrecht) B 92, 330 (1977).
[7] R. L. Carlin, K. O. Joung, A. Paduan Filho, C. J. O'Connor, and E. Sinn, J. Phys. C 12, 293 (1979).

[8]F. W. Klaaijsen, Z. Dokoupil, and W. J. Huiskamp, Physica (Utrecht) B **79**, 547 (1975); F. W. Klaaijsen, thesis, Leiden, 1974.
[9]D. P. Freyberg, G. M. Mockler, and E. Sinn, J. Chem. Soc. Dalton Trans. **1976**, 447.
[10]P. W. R. Corfield, R. J. Doedens, and J. A. Ibers, Inorg. Chem. **6**, 197 (1967).
[11]A. M. Greenaway and E. Sinn, J. Am. Chem. Soc. **100**, 8080 (1978).
[12]D. T. Cromer and J. T. Waber, *International Tables for X-ray Crystallography* (Kynoch, Birmingham, England, 1974), Vol. IV; A. F. Stewart, E. R. Davidson, and W. T. Simpson, J. Chem. Phys. **42**, 3175 (1975).
[13]D. T. Cromer and J. A. Ibers, *International Tables for X-ray Crystallography* (Kynoch, Birmingham, England, 1974), Vol. IV, Table 2.3.
[14]P. C. Healy, G. M. Mockler, D. P. Freyberg, and E. Sinn, J. Chem. Soc. Dalton Trans. **1975**, 671.
[15]See AIP document no. PAPS JCPSA-75-430-3 for 3 pages of observed and calculated structure factors. Order by PAPS number and journal reference from American Institute of Physics, Physics Auxiliary Publication Service, 335 East 45th Street, New York, N. Y. 10017. The price is $1.50 for each microfiche or $5 for photocopies. Airmail is additional. Make checks payable to the American Institute of Physics.
[16]H. den Adel, thesis, Leiden (in preparation).
[17]C. Domb and A. R. Miedema, Prog. Low Temp. Phys. **4**, 296 (1964).
[18]D. W. Engelfriet, W. L. Groeneveld, H. A. Groenendijk, J. J. Smit, and G. M. Nap, Z. Naturforsch. Teil A **35**, 115 (1980).
[19]M. F. Sykes and M. E. Fisher, Physica (Utrecht) **28**, 919 (1962).
[20]M. E. Fisher, J. Math. Phys. **4**, 124 (1963).
[21]M. F. Sykes, D. S. Gaunt, P. D. Roberts, and J. A. Wyles, J. Phys. A **5**, 624 (1972).
[22]R. Navarro and L. J. de Jongh, Physica (Utrecht) B **94**, 67 (1978).
[23]M. E. Fisher, Rep. Prog. Phys. **30**, 615 (1968).
[24]T. Moriya, Phys. Rev. **120**, 91 (1960).
[25]I. F. Silvera, J. H. M. Thornley, and M. Tinkham, Phys. Rev. Sect. A **136**, 695 (1964).
[26]D. B. Losee, J. N. McElearney, G. E. Shankle, R. L. Carlin, P. J. Cresswell, and W. T. Robinson, Phys. Rev. B **8**, 2185 (1973); S. N. Bhatia, C. J. O'Connor, and R. L. Carlin, Inorg. Chem. **15**, 2900 (1976).
[27]A. Herweijer, W. J. M. de Jonge, A. C. Botterman, A. L. M. Bongaarts, and J. A. Cowen, Phys. Rev. B **5**, 4618 (1972).
[28]J. N. McElearney and S. Merchant, Phys. Rev. B **18**, 3612 (1978).
[29]M. Karnezos, G. Lecomte, and S. A. Friedberg, J. Appl. Phys. **50**, 1856 (1979).
[30]A. J. van Duyneveldt (private communication).
[31]R. D. Spence and A. C. Botterman, Phys. Rev. B **9**, 2993 (1974); H. A. Groenendijk and A. J. van Duyneveldt (to be published).